Elastic α − ^{12}C Scattering and the $^{12}C(\alpha,\gamma)^{16}O$ $E2$ S Factor

P. Tischhauser,[1] R. E. Azuma,[2] L. Buchmann,[3] R. Detwiler,[1] U. Giesen,[1,3] J. Görres,[1] M. Heil,[4] J. Hinnefeld,[5] F. Käppeler,[4] J. J. Kolata,[1] H. Schatz,[1,6] A. Shotter,[7] E. Stech,[1] S. Vouzoukas,[1] and M. Wiescher[1]

[1]*University of Notre Dame, Notre Dame, Indiana*
[2]*University of Toronto, Toronto, Ontario, Canada*
[3]*TRIUMF, Vancouver, British Columbia, Canada*
[4]*Forschungszentrum Karlsruhe, Karlsruhe, Germany*
[5]*Indiana University of South Bend, South Bend, Indiana*
[6]*Michigan State University, East Lansing, Michigan*
[7]*University of Edinburgh, Edinburgh, United Kingdom*

(Received 6 September 2001; published 31 January 2002)

Angular distributions of $^{12}C(\alpha,\alpha)^{12}C$ have been measured for $E_\alpha = 2.6-8.2$ MeV, at angles from 24° to 166°, yielding 12 864 data points. R-matrix analysis of the ratios of elastic scattering yields a reduced width amplitude of $\gamma_{12} = 0.47 \pm 0.06$ MeV$^{1/2}$ for the $E_x = 6.917$ MeV (2^+) state in ^{16}O ($a = 5.5$ fm). The dependence of the χ^2 surface on the interaction radius a has been investigated and a deep minimum is found at $a = 5.42^{+0.16}_{-0.27}$ fm. Using this value of γ_{12}, radiative α capture and ^{16}N β-delayed α-decay data, the S factor is calculated at $E_{\text{c.m.}} = 300$ keV to be $S_{E2}(300) = 53^{+13}_{-18}$ keV b for destructive interference between the subthreshold resonance tail and the ground state $E2$ direct capture.

DOI: 10.1103/PhysRevLett.88.072501 PACS numbers: 26.30.+k, 25.40.Ny, 26.50.+x

During stellar helium burning, the two most important reactions are triple-α and $^{12}C(\alpha,\gamma)^{16}O$. The relative rates of these two reactions determine the C/O ratio and set the stage for future stellar evolution [1]. A reliable extrapolation of the reaction rate of $^{12}C(\alpha,\gamma)^{16}O$ from measured cross sections at $E_{\text{c.m.}} \geq 1.0$ MeV to stellar helium burning temperatures ($E_{\text{c.m.}} = 300$ keV) has been a long-standing problem. Analysis is complicated by the separate energy dependence of the electric dipole ($E1$) and quadrupole ($E2$) transitions to the ground state. While the lowest-energy experimental cross sections of $^{12}C(\alpha,\gamma)^{16}O$ are dominated by a broad 1^- resonance at $E_{\text{c.m.}} = 2.42$ MeV, it is the influence of two subthreshold states bound by 45 (1^-) and 245 keV (2^+) which determines the cross section at the energy of interest usually expressed as the S factor $S(300)$. Extrapolations are further complicated by the interference of direct capture with the resonant $E2$ contribution, and the evidence of cascade transitions through excited states of ^{16}O, albeit with lower cross sections than the ground state transitions.

By measuring the β-delayed α-decay spectrum of ^{16}N [2] it has been possible to constrain the $E1$ portion of $^{12}C(\alpha,\gamma)^{16}O$. These data were combined with elastic scattering phase shifts [3] and $^{12}C(\alpha,\gamma)^{16}O$ cross section data [4–7] in an R-matrix fit yielding $S_{E1}(300) = 79 \pm 21$ keV b [2]. While the uncertainty of the $E1$ contribution has thus been reduced to 25%, the ^{16}N data cannot constrain the $E2$ contribution. A recent global R-matrix fit to the relevant primary data [8] yielded a similar $S_{E1}(300)$ value, and an estimate of $S_{E2}(300)$ at 70 ± 70 keV b. Fitting secondary quantities like elastic scattering phase shifts ignores inherent correlations between these quantities [8].

Extremely low cross sections [$\sigma(300) \approx 10^{-17}$ b] make a direct measurement of $^{12}C(\alpha,\gamma)^{16}O$ increasingly difficult for $E_{\text{c.m.}} < 1$ MeV [4–7]. Elastic scattering measurements have been suggested [3,8] as an alternative method to constrain the $E2$ cross section. The $E2$ part of the $^{12}C(\alpha,\gamma)^{16}O$ cross section is largely, though not entirely (see below), determined by the reduced width amplitude γ_{12} of the subthreshold 2^+ state which can be obtained by global fits to the elastic scattering data. (For R-matrix expressions and notations see Refs. [2,8]. γ_{12} is the reduced width amplitude of the first state with angular momentum $\ell = 2$, corresponding to the $E_x = 6.917$ MeV state in ^{16}O.) While several measurements [3,9–19] of $^{12}C(\alpha,\gamma)^{12}O$ have been made in the past, only a few have provided phase shift error bars [3,9], and only one [3] has made the primary data available [20]. It has been shown, however, in [8] that the data set of [3] has limitations both in the experiment as well as in the phase shift analysis performed in [3], which has also been noticed in [21]. A new elastic scattering experiment has therefore been performed at the University of Notre Dame.

The 10-MV FN tandem accelerator at the University of Notre Dame provided up to 200 nA of highly collimated $^4He^{2+}$ beam on carbon target foils. The beam was positioned on the target using a pair of 2 mm slits outside of the chamber, restricting the beam's angular divergence to less than 0.09°, and fixing the position of the beam spot within 1.5 mm. The beam current was integrated on a Faraday cup behind the chamber. Beam energies were calibrated to 0.1% using the narrow ^{16}O states at $E_\alpha = 3.577$ (2^+) and 5.245 (4^+) MeV [22], and beam energies were repeatable to the same precision. Beam energies were confirmed, in addition, by analyzing Au and ^{12}C elastic peak centroids.

Natural carbon targets were used, each with a thin (1–2 μg/cm^2) layer of evaporated Au, and carbon thicknesses of 8–25 μg/cm^2. The targets were oriented at a 45° angle relative to the incident beam. The target thickness was monitored by comparing yields relative to ^{197}Au$(\alpha,\alpha)^{197}$Au, and showed that targets experienced an increase of 10%–40% in thickness over time. Corrections for the target thickness growth were applied in the analysis.

An array of 32 ion-implanted silicon detectors (100 μm thickness, 100 mm^2 area) were arranged at a distance of 62 cm from the target at the center of a 2 m diameter vacuum chamber. The array covered an angular range of 24°–166°. The position of each detector was aligned using a telescope. The uncertainty in angular position was less than 0.1°. To monitor possible systematic effects, half of the detectors were located forward of the target, while the other half were positioned behind it. The two sets of detectors overlapped in angular range. This arrangement allowed for a comparison of "left" vs "right" yields which were found to agree very well. A pair of collimators in front of each detector served to define the solid angle and restrict off-axis particles. The detector and target positions remained fixed throughout all runs. The ability to collect all angular distribution data in a single run constituted a major improvement over [3]. The detector array was connected to a modular system of preamplifiers and amplifiers described in Ref. [23]. The resolution of a typical detector was 20 keV. Data were taken in an event-by-event mode. Electronic dead times were monitored with pulsers connected to each detector channel.

Angular distributions were obtained at 402 energies between 2.6 and 8.2 MeV, resulting in 12 864 spectra. All resonances below 8.2 MeV were scanned. Narrow resonances proved valuable for determining the target thickness integration procedure. For energies below the proton threshold $E_\alpha \approx 6.62$ MeV, elastic peak shapes, given by kinematics and geometry, prevented the separation of scattered α's from ^{12}C and ^{13}C for angles below 40°. Excluding angles below 40° from the fits did not influence the final results.

It has been shown in Ref. [8] that the energy-angle surface of the elastic scattering cross section in $^{12}\mathrm{C} + \alpha$ is highly structured. This structure is directly related to the resonance properties of $^{12}\mathrm{C} + \alpha$ and is independent of the absolute cross section. It was decided to fit the ratios of experimental yields, calculated by dividing the yield at each angle by the yield of a given angle (the "reference angle"). This normalization removes (to first order) the dependence on target thickness and beam current integration. However, because errors associated with the reference angle are unduly weighted in such an analysis, we construct a total χ^2 by summing the respective partial χ_i^2 for all possible reference angles.

Since $^{12}\mathrm{C}(\alpha,\alpha)^{12}\mathrm{C}$ has several resonances with small widths ranging from sub-keV to several tens of keV, the cross section was convoluted over the target thickness and beam energy resolution. The convolution was performed independently using three different convolution kernels (modeled on results from sub-keV-width resonances), with nearly identical results. The *R*-matrix fits were done using a single channel approach as described in [8], but a multichannel program has been employed as well [24] for the higher energy data. Many of the results here are for an interaction radius of $a = 5.5$ fm; however, the effects of different values of a are explored below.

For reason of computing speed most of the fits were conducted with the elastic channel only in the fit program and with a set of 356 distributions below the proton threshold. These fits included all known resonances up to 6.4 MeV laboratory energy and also all subthreshold states above $E_x = 6$ MeV in ^{16}O. Results with a multichannel program indicated, however, that states above the particle threshold influence the results. In the single channel program, the elastic partial widths for states above threshold were fixed to values based on multichannel fits. Subthreshold widths were then found to be similar in both kinds of fits. Partial waves of $\ell = 0$ to $\ell = 6$ were fitted. Boundary conditions were set using the energies of subthreshold resonances in ^{16}O for $\ell = 0$ to $\ell = 3$, the narrow $E_{\mathrm{c.m.}} = 3.933$ MeV resonance for $\ell = 4$, and $E_{\mathrm{c.m.}} = 1.0$ MeV for $\ell = 5$ and 6, respectively. Thirty-two *R*-matrix parameters were employed in the single channel program, while additional experimental parameters describe the properties of the 10 targets used. Figure 1 presents the

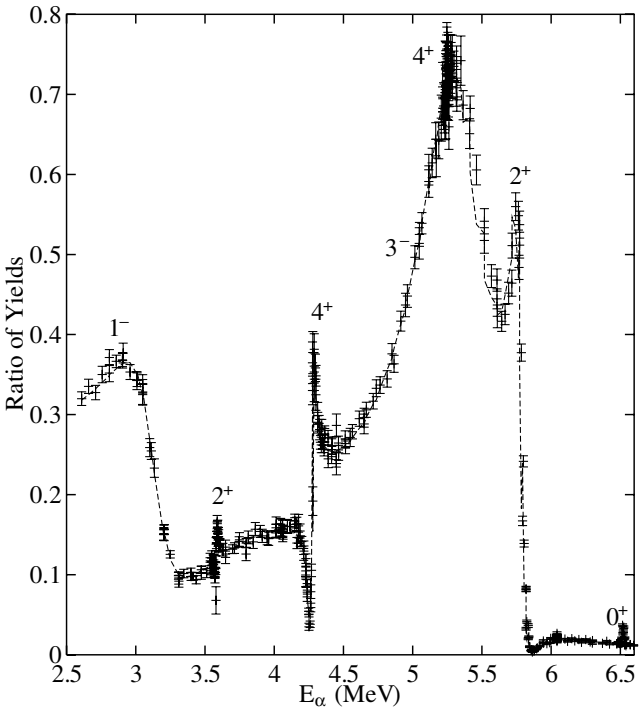

FIG. 1. Excitation curve of the yield ratio for $\theta_{\mathrm{lab}} = 84.0°$ and $\theta_{\mathrm{lab}} = 58.9°$ and best fit at $a = 5.5$ fm. The errors shown are statistical only.

ratios of the excitation function for $\theta_{\rm lab} = 84.0°$ relative to the one at $\theta_{\rm lab} = 58.9°$ and a fit to this function.

The best fit for the reduced width amplitude of the 2^+ subthreshold state occurred for $\gamma_{12} = 0.47$ MeV$^{1/2}$, with $\gamma_{11} = 0.27$ MeV$^{1/2}$ for the subthreshold 1^- state for the single channel program. Identical results were obtained in the multichannel program (both $a = 5.5$ fm). To obtain an error estimation, fits were obtained for values of γ_{12} from 0.2 to 0.60 MeV$^{1/2}$, with all other parameters being allowed to vary. The resulting χ^2 curve is shown in Fig. 2(a). The same approach was used to scan γ_{11} from 0 to 0.60 MeV$^{1/2}$ for the 1^- state. A 1σ uncertainty of $\gamma_{12} = 0.47 \pm 0.06$ MeV$^{1/2}$, and $\gamma_{11} = 0.27^{+0.11}_{-0.27}$ MeV$^{1/2}$ was calculated with the previously established [2] guideline $\chi^2 < \chi^2_{\rm min} \pm 9\chi^2_\nu$. A list of the best fit parameters is presented in Table I. The best fit has a χ^2_ν of approximately 1.66. Deviations from an ideal fit occur at resonances with widths in the keV range where the sensitivity to target effects and beam energy calibration is most pronounced.

The influence of the interaction radius a on the results has been investigated. A strong dependence of χ^2 as a function of a was found with $a = 5.42^{+0.16}_{-0.27}$ fm as the best value shown in Fig. 2(b). The dependence of γ_{12} on the interaction radius a is shown in Fig. 3. The width decreases, as expected, with increasing a. Close to the minimum an approximate $\frac{1}{a}$ dependence is found for γ_{12} and other widths. This result justifies using $a = 5.5$ fm throughout the analysis and represents the first real restriction on the interaction radius a in the $^{12}C(\alpha,\gamma)^{16}O$ problem.

Previous extrapolations of $S_{E2}(300)$ have been made using simultaneous fits to all available primary data [8]. Direct inclusion of all the elastic scattering data presented here will statistically dominate other data sets. For this reason, the reduced width amplitude γ_{12} can be directly fixed within its errors in such fits without significantly narrowing the χ^2 range estimated in the minimization. Therefore the best-fit elastic scattering parameters for the 2^+ states were combined with radiative capture data [4–7] from $^{12}C(\alpha,\gamma)^{16}O$ and ^{16}N data [2]. This analysis leads to a value of $S_{E1}(300) = 80 \pm 20$ keV b, and $S_{E2}(300) = 49^{+7}_{-9}$ or 58^{+8}_{-11} keV b, depending on the sign of the $E = 4.39$ MeV 2^+ resonance γ width amplitude relative to that for direct capture and the subthreshold resonance. As this interference sign is unknown, the two results are averaged and errors include the limits on both measurements, yielding $S_{E2}(300) = 53 \pm 13$ keV b. With the full range of a allowed here, the final result is $S_{E2}(300) = 53^{+13}_{-18}$ keV b. In this analysis destructive interference between the ground state direct capture and the tail of the subthreshold 2^+ resonance has been employed. This is justified by a total decrease in χ^2 of nearly 300 between the destructive and constructive options, largely due to the γ-angular distributions of Refs. [5] and [7]. However, additional angular distributions would be desirable, as the constructive option leads to 92 and 102 keV b, respectively, for $S_{E2}(300)$. The data set of Ref. [25] is unfortunately not available to the authors.

The current value of the reduced width amplitude $\gamma_{12} = 0.47 \pm 0.06$ MeV$^{1/2}$ agrees with the original phase shift analysis of Ref. [3], which yielded $\gamma_{12} = 0.48 \pm 0.06$ MeV$^{1/2}$ for $a = 5.43$ fm. However, the current value has many of the restrictions on R-matrix parameters removed which were applied in Ref. [3]. A recent sub-Coulomb α-transfer experiment [26] involving both ^{6}Li and ^{7}Li beams came to $\gamma_{12} = 0.33 \pm 0.03$ MeV$^{1/2}$ at $a = 5.5$ fm. A similarly lower value of $\gamma_{12} = 0.36 \pm 0.06$ MeV$^{1/2}$ would have been found here,

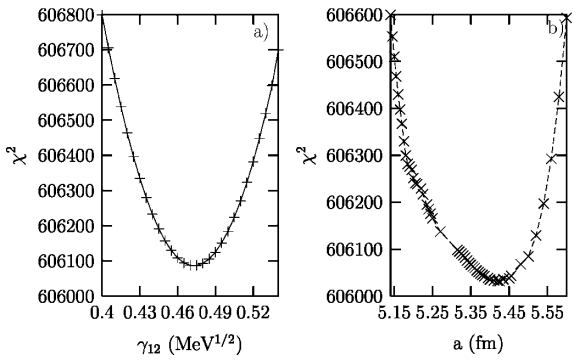

FIG. 2. (a) χ^2 minimization for γ_{12} at $a = 5.5$ fm, and (b) χ^2 minimization for the interaction radius a.

TABLE I. Best fit R-matrix parameters for $a = 5.5$ fm. Energies in brackets are fixed to their physical value.

$\gamma_{\lambda\ell}$	(MeV$^{1/2}$)	$E_{\lambda\ell}$ (MeV)	
γ_{10}	9.82×10^{-7}	E_{10}	(-1.1130)
γ_{20}	9.198×10^{-3}	E_{20}	4.888
γ_{30}	0.865	E_{30}	9.67
γ_{11}	0.270	E_{11}	(-0.0451)
γ_{21}	0.555	E_{21}	3.358
γ_{31}	2.74	E_{31}	52.7
γ_{41}	0.139[a]	E_{41}	5.350[a]
γ_{12}	0.473	E_{12}	(-0.2450)
γ_{22}	2.43×10^{-2}	E_{22}	2.684
γ_{32}	8.95×10^{-2}	E_{32}	4.387
γ_{42}	2.60	E_{42}	44.5
γ_{52}	0.128[a]	E_{52}	5.978[a]
γ_{13}	0.190	E_{13}	(-1.032)
γ_{23}	0.471	E_{23}	5.63
γ_{33}	18.7	E_{33}	2.90×10^3
γ_{14}	0.44	E_{14}	3.196
γ_{24}	3.09×10^{-2}	E_{24}	3.936
γ_{34}	1.287	E_{34}	13.31
γ_{15}	0.67	E_{15}	7.845
γ_{16}	0.29	E_{16}	6.0[b]

[a]From phase-shift fit. Fixed in minimization.
[b]Set limit.

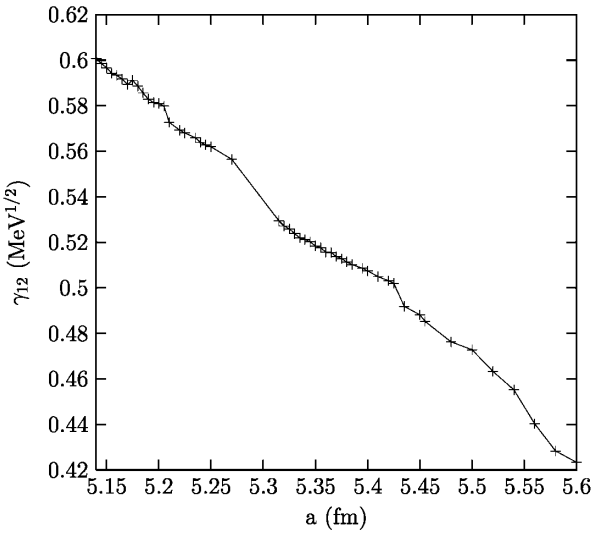

FIG. 3. Dependence of γ_{12} on the interaction radius a for the minimization shown in Fig. 2(b).

if the high lying $E_x = 13.02$ MeV 2^+ state in ^{16}O had not been included in this analysis. The present $S_{E2}(300)$ value of 53^{+13}_{-18} keV b agrees with the value of 36 ± 6 keV b previously derived from a fit using the energy dependence of a cluster model matched to the experimental cross section of Ref. [7]. The value is also consistent with the microscopic-model analysis of [5], which estimated $S_{E2}(300)$ as 80 ± 25 keV b, and the range 50–200 keV b cited in [27]. It also agrees with a recent analysis of radiative cascade data through the 6.9 MeV state [28]. The NACRE collaboration value of $S_{E2}(300) = 120$ keV b [29] is outside our limits. However, the question of interference signs in the $E2$ radiative capture warrants further investigation.

Combining the $S_{E1}(300)$ and $S_{E2}(300)$ values along with an estimation [8] of the cascade transitions of $S_{\text{case}}(300) = 16 \pm 16$ keV b [27,28,30], a value of $S(300) = 149 \pm 29$ keV b is found. This agrees very well with the total recommended value of $S(300) = 146$ keV b in Ref. [30]. Therefore the stellar reaction rates and approximations to this rate in Ref. [30] can be used without modification.

[1] T. A. Weaver and S. E. Woosley, Phys. Rep. **227**, 65–93 (1993).
[2] R. E. Azuma *et al.,* Phys. Rev. C **50**, 1194 (1994).
[3] R. Plaga *et al.,* Nucl. Phys. **A465**, 291 (1987).
[4] P. Dyer and C. A. Barnes, Nucl. Phys. **A233**, 495 (1974).
[5] A. Redder *et al.,* Nucl. Phys. **A462**, 385 (1987).
[6] R. M. Kremer *et al.,* Phys. Rev. Lett. **60**, 1475 (1988).
[7] J. M. L. Ouellet *et al.,* Phys. Rev. C **54**, 1982 (1996).
[8] L. Buchmann *et al.,* Phys. Rev. C **54**, 393 (1996).
[9] M. D'Agostino Bruno *et al.,* Nuovo Cimento A **27**, 1 (1975).
[10] R. W. Hill, Phys. Rev. **90**, 845 (1953).
[11] J. W. Bittner and R. D. Moffat, Phys. Rev. **96**, 374 (1954).
[12] C. M. Jones *et al.,* Nucl. Phys. **37**, 1 (1962).
[13] J. D. Larson and T. A. Tombrello, Phys. Rev. **147**, 760 (1966).
[14] G. J. Clark *et al.,* Nucl. Phys. **A110**, 481 (1968).
[15] J. M. Morris *et al.,* Nucl. Phys. **A112**, 97 (1968).
[16] T. P. Marvin and P. P. Singh, Nucl. Phys. **A180**, 282 (1972).
[17] F. Brochard *et al.,* J. Phys. (Paris) **36**, 113 (1975).
[18] A. D. Frawley *et al.,* Phys. Rev. C **25**, 2935 (1982).
[19] M. A. Kovash *et al.,* Phys. Rev. C **31**, 1065 (1985).
[20] R. Plaga, Diplomarbeit, Universität Münster, 1986.
[21] C. Angulo and P. Descouvemont, Phys. Rev. C **61**, 064611 (2000).
[22] D. R. Tilley *et al.,* Nucl. Phys. **A564**, 1 (1993).
[23] S. L. Thomas *et al.,* Nucl. Instrum. Methods Phys. Res., Sect. A **288**, 212 (1990).
[24] L. Buchmann *et al.* (to be published).
[25] R. Kunz *et al.,* Phys. Rev. Lett. **86**, 3244 (2001).
[26] C. R. Brune *et al.,* Phys. Rev. Lett. **83**, 4025 (1999).
[27] F. C. Barker and T. Kajino, Aust. J. Phys. **44**, 396 (1991).
[28] L. Buchmann, Phys. Rev. C **64**, 022801(R) (2001).
[29] NACRE Collaboration, C. Angulo *et al.,* Nucl. Phys. **A656**, 3 (1999).
[30] L. Buchmann, Astrophys. J. **468**, L127 (1996); **479**, L153 (1997).